Critical Point of an Interacting Two-Dimensional Atomic Bose Gas

Peter Krüger, Zoran Hadzibabic, Jean Dalibard

Critical Point of an Interacting Two-Dimensional Atomic Bose Gas

Peter Krüger, Zoran Hadzibabic, and Jean Dalibard
Laboratoire Kastler Brossel, Ecole Normale Supérieure, 24 rue Lhomond, 75005 Paris, France
(Dated: 8th March 2007)

We have measured the critical atom number in a harmonically trapped two-dimensional (2D) Bose gas of rubidium atoms at different temperatures. We found this number to be about five times higher than predicted by the semi-classical theory of Bose-Einstein condensation (BEC) in the ideal gas. This demonstrates that the conventional BEC picture is inapplicable in an interacting 2D atomic gas, in sharp contrast to the three-dimensional case. A simple heuristic model based on the Berezinskii-Kosterlitz-Thouless theory of 2D superfluidity and the local density approximation accounts well for our experimental results.

PACS numbers: 03.75.Lm, 32.80.Pj, 67.40.-w

Bose-Einstein condensation (BEC) at a finite temperature is not possible in a homogeneous two-dimensional (2D) system, but an interacting Bose fluid can nevertheless become superfluid at a finite critical temperature [1]. This phase transition is described by the Berezinskii-Kosterlitz-Thouless (BKT) theory [2, 3], and is unconventional because it does not involve any spontaneous symmetry breaking and emergence of a uniform order parameter. It is instead associated with a topological order embodied in the pairing of vortices with opposite circulations; true long-range order is destroyed by long wavelength phase fluctuations even in the superfluid state [4, 5].

Recent advances in producing harmonically trapped, weakly interacting (quasi-)2D atomic gases [6, 7, 8, 9, 10, 11, 12, 13, 14] have opened the possibility for detailed studies of BKT physics in a controllable environment. There has been some theoretical debate on the nature of the superfluid transition in these systems [15, 16, 17, 18, 19] because the harmonic confinement modifies the density of states compared to the homogenous case. This allows for "conventional" finite temperature Bose-Einstein condensation in the *ideal* 2D gas [20]. Early experiments have been equally consistent with the BEC and the BKT picture of the phase transition. For example, the density profiles at very low temperatures [6] are expected to be the same in both cases. However, recent studies of matter wave interference of independent 2D atomic clouds close to the transition have revealed both thermally activated vortices [12, 13] and quasi-long-range coherence properties [13] in agreement with the BKT theory [21, 22].

In this Letter, we study the critical atom number in a 2D gas of rubidium atoms, and observe stark disagreement with the predictions of the ideal gas BEC theory. We detect the critical point by measuring independently (i) the onset of bimodality in the atomic density distribution and (ii) the onset of interference between independent 2D clouds. These two measurements agree with each other, and for a range of temperatures $T \approx 50$–$110\,\mathrm{nK}$ give critical atom numbers N_c which are

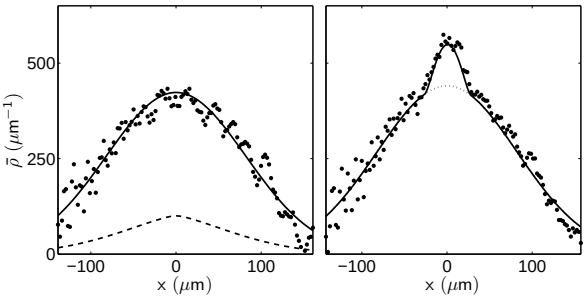

Figure 1: Phase transition in a rubidium 2D gas. 2D clouds confined parallel to the xy plane are released from an optical lattice and the density distribution is recorded by absorption imaging along y after $t = 22\,\mathrm{ms}$ of time of flight. The measured line densities $\bar{\rho}(x)$ (•) for an atom number just below (left) and just above (right) the critical number are displayed together with bimodal fits (solid lines). The dashed line in the left panel shows the expected distribution of the 2D ideal gas at the threshold of conventional BEC in our lattice potential at the same temperature ($T = 92\,\mathrm{nK}$). The dotted line in the right panel indicates the Gaussian part of the bimodal distribution.

~ 5 times higher than the ideal gas prediction for conventional Bose-Einstein condensation in our trap [20]. For comparison, in three-dimensional (3D) atomic gases, where conventional BEC occurs, the increase of the critical atom number due to repulsive interactions is typically on the order of ten percent [23, 24]. We construct a simple heuristic model based on the BKT theory of 2D superfluidity and the local density approximation, which gives good agreement with the experimental results.

In [13] we studied quasi-long-range coherence of a trapped 2D gas, which is directly related to the *superfluid* density ρ_s [22]. In that case, signatures of the BKT transition emerge only once a significant part of the cloud becomes superfluid. Since the atomic density in the trap is not uniform, this happens slightly below the true critical temperature for the onset of superfluidity in the trap center, and the observed transition is rounded off. The present study concentrates on the exact critical point and relates to the *total* density at criticality ρ_c, which has been of long standing theoretical interest [25, 26].

Our experimental procedure for the preparation of cold 2D Bose gases has been described in [13]. We start with a ^{87}Rb 3D condensate in a cylindrically symmetric magnetic trap with trapping frequencies $\omega_x = 2\pi \times 10.6\,\mathrm{Hz}$ and $\omega_y = \omega_z = 2\pi \times 125\,\mathrm{Hz}$. Adding a blue detuned one-dimensional (1D) optical lattice with a period of $d = 3\,\mu$m along the vertical direction z splits the sample into a few independent clouds and compresses them into the 2D regime. The lattice is formed by two laser beams at $\lambda = 532\,\mathrm{nm}$ propagating in the yz plane, intersecting at a small angle and focussed to waists of about $120\,\mu$m. The peak depth of the lattice is $h \times 35\,\mathrm{kHz}$, corresponding to a vertical confinement of $\omega_z = 2\pi \times 3.0\,\mathrm{kHz}$. The interaction strength is $g = (\hbar^2/m)\tilde{g}$, where the dimensionless coupling constant $\tilde{g} = a_s\sqrt{8\pi m\omega_z/\hbar} = 0.13$, $a_s = 5.2\,\mathrm{nm}$ is the scattering length, and m the atomic mass [15, 27]. For all experiments reported here both chemical potential μ and temperature T satisfy the 2D criteria $\mu, kT < \hbar\omega_z$. The finite waists of the lattice beams result in a slow variation of ω_z along x; the variation of the zero point energy $\hbar\omega_z/2$ modifies ω_x to $2\pi \times 9.4\,\mathrm{Hz}$ at the trap center.

We measure the critical atom number in the 2D gas by varying the total atom number N at a fixed temperature. We start with a highly degenerate 2D sample and keep it trapped for a time τ varying between 1 and 10 s. During this time we maintain a constant temperature by balancing the residual heating due to inelastic collisions with evaporative cooling. Evaporation is induced by a constant radio frequency field in the range of 10–25 kHz above the frequency corresponding to the bottom of the trap. When the waiting time τ increases, the atom number gradually drops below the critical value.

The atomic density profiles are recorded in the xz plane by resonant absorption imaging along the shorter axis of the cloud y after $t = 22\,\mathrm{ms}$ of time of flight expansion. Along z the profiles are Gaussian with a width corresponding to the single particle ground state along that direction. Along x, we find that for all atom numbers below the critical number N_c a Gaussian distribution fits the data well, whereas the ideal gas model would predict a distribution that is much more peaked at the center of the cloud (Fig. 1). For $N > N_c$, the profiles exhibit a clearly bimodal shape. For the subsequent analysis, a bimodal function consisting of the sum of a Gaussian and an inverted parabola (Thomas-Fermi profile) is fitted to the experimental data. We use the fit results to assign to each image a total atom number N, a number N_0 of atoms within the Thomas-Fermi part of the distribution, and a temperature T (from the width of the Gaussian along x). The atom number determination takes into account the detection efficiency of the imaging system that has been calibrated by measuring critical atom numbers for 3D BECs [23, 24]. We estimate the systematic uncertainties of our atom number and temperature calibrations to be 20% and 10%, respectively. The measured temperatures scale linearly with the energy of the evaporation surfaces $E_{\mathrm{evap}} = \eta kT$, with a truncation parameter $\eta \approx 10$, compatible with the usual 3D values.

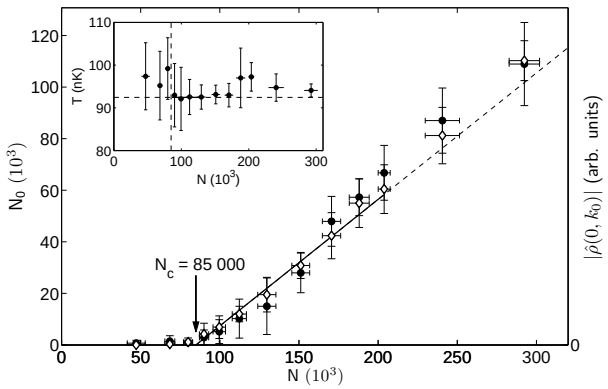

Figure 2: Measurement of the critical point. The number of atoms in the Thomas-Fermi part of the bimodal distribution N_0 ($\diamond$) is plotted as a function of the total atom number N. The solid line shows the extrapolation we use to determine N_c. For comparison, the interference amplitude $|\hat{\rho}(0,k_0)|$ ($\bullet$) is also displayed as a function of N. It shows the same threshold N_c within our experimental precision. The inset shows that the temperature is to a good approximation constant for all data points. Horizontal and vertical dashed lines indicate the average temperature and the critical atom number, respectively. The solid line marks the region used to determine the average temperature $T = 92(6)\,\mathrm{nK}$ close to the transition. Each data point is based on 5–10 images, all error bars represent standard deviations.

Fig. 2 illustrates the threshold behavior of N_0 as a function of the total atom number N [28], and Fig. 3 displays the measured threshold values N_c at four different temperatures. The ideal gas theory of conventional Bose-Einstein condensation predicts the critical number in a single 2D gas [20]:

$$N_{c,\mathrm{id}} = \frac{\pi^2}{6}\left(\frac{kT}{\hbar\bar{\omega}}\right)^2 , \qquad (1)$$

where $\bar{\omega}$ is the geometric mean of the two trapping frequencies in the plane. For comparison with our experimental results we need to account for the occupation of multiple lattice planes. For this purpose we have numerically integrated the Bose-Einstein distribution for our experimental configuration (magnetic trap and lattice potential). We assume that the planes have a common temperature and chemical potential because high energy thermal atoms ensure thermal contact between them (the minimum of the potential barrier is $k \times 460\,\mathrm{nK}$) [29]. Our calculation also includes several smaller effects. First, it accounts for the finiteness of the lattice beam waists, beyond the modification of ω_x mentioned above. Second, it includes the small occupation of the excited states along z, which results from the fact that $\hbar\omega_z/(kT)$ is finite. Finally, the result depends on a ten percent level on the exact position of the lattice planes relative to the minimum

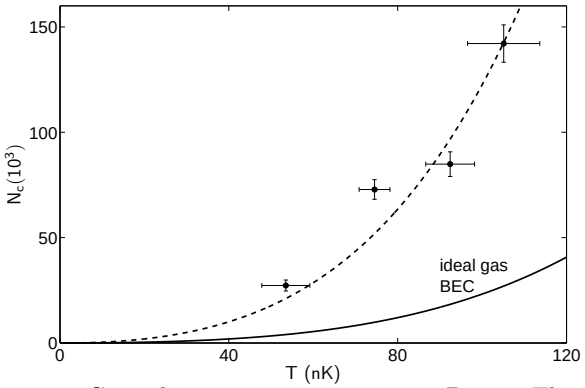

Figure 3: Critical point in an interacting 2D gas. The critical atom number N_c (•) is measured at four different temperatures T. Displayed error bars are statistical. The solid line shows the ideal 2D gas BEC prediction $N_{c,id}^{multi}$. The dashed line is the best empirical fit to the data, which gives $N_c = \alpha\, N_{c,id}^{multi}$ with $\alpha = 5.3(5)$.

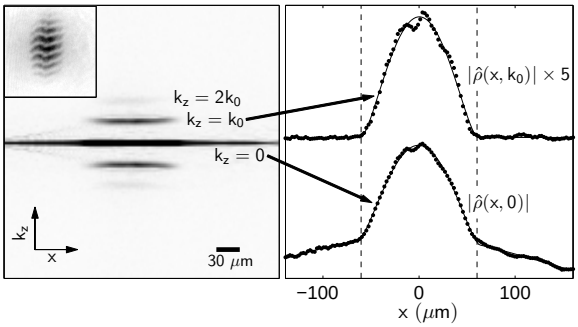

Figure 4: Coherence and density profile below the transition. Interference of 2D clouds is used to compare the coherent part of the cloud with the part following the Thomas-Fermi density distribution. Left: Interference patterns in the xz plane (see example in inset) are Fourier transformed along the expansion axis z and averaged over ten images taken under identical conditions, to obtain $|\hat{\rho}(x, k_z)|$. Right: Within experimental precision, fits to the total density profile $|\hat{\rho}(x, 0)|$ and the interference amplitude profile $|\hat{\rho}(x, k_0)|$ give the same Thomas-Fermi diameter $2R_{TF}$, indicated by the dashed lines. The weak second harmonic peak at $k_z = 2k_0$ reveals small occupation of the outer lattice planes.

of the magnetic trap potential. Since we do not fully control this position, we average over the possible configurations. We obtain the result $N_{c,id}^{multi} = pN_{c,id}$, where the effective number of planes p smoothly grows with temperature, from ≈ 2.2 at 50 nK to ≈ 4.2 at 110 nK. The resulting $N_{c,id}^{multi}(T)$ is shown in Fig. 3 as a solid line.

Our measurements clearly show systematically higher N_c than expected for ideal gas condensation. We display an empirical fit to the data according to $\alpha N_{c,id}^{multi}(T)$ where the scaling factor α is the only free parameter. We find that our data is consistent with the functional temperature scaling $N_{c,id}^{multi}(T)$, but the experimental values for N_c are a factor of $\alpha = 5.3(5)$ higher, where the quoted error is statistical.

We also study the coherent fraction of the 2D gas and compare its behavior with the bimodal density profiles. We investigate the interference patterns that form after releasing the independent planar gases from the trap (Fig. 4) [13]. Fourier transforming the density profile $\rho(x, z) \rightarrow \mathcal{F}[\rho(x, z)] \equiv \hat{\rho}(x, k_z)$ allows us to quantify the size of the coherent, i.e. interfering part of the gas as a function of N. The spatial frequency corresponding to the fringe period for the interference of neighboring planes is $k_0 = md/\hbar t$. We find that $\hat{\rho}(x, k_0)$ is well fitted by a pure Thomas-Fermi profile. Within our experimental accuracy, the radii $R_{TF}(k_0)$ of these profiles are equal to those obtained from a bimodal fit to the density. In particular, the onset of interference coincides with the onset of bimodality (circles and diamonds in Fig. 2, respectively).

We now turn to the interpretation of our measurements in the framework of the BKT theory of 2D superfluidity. The theory predicts a universal jump of the *superfluid* density at the transition, from $\rho_s = 0$ to $\rho_s\lambda^2 = 4$ [21] (for experiments see [1, 13]). However, the *total* density at the critical point, $\rho_c > \rho_s$, is not universal because it depends on the microscopic interactions. For weak interactions ($\tilde{g} < 1$),

$$\rho_c = -\frac{1}{\lambda^2} \ln\left(C/\tilde{g}\right) \ , \qquad (2)$$

where C is a dimensionless constant [25]. High-precision Monte Carlo calculations give $C = 380 \pm 3$ [26]. For our value of $\tilde{g} = 0.13$ (experimentally confirmed by measuring R_{TF} as a function of N_0) we obtain $\rho_c\lambda^2 = 8.0$.

In a harmonic trap the transition is expected to occur when the density in the center of the cloud reaches the critical value ρ_c. The corresponding critical number $N_{c,BKT}$ can be calculated in the local density approximation, but the result clearly depends on the shape of the density distribution. For simplicity, we restrict our analysis to a single plane, and consider two different models. Theoretically, a first good candidate is the self-consistent Hartree-Fock (HF) density profile [19] (see also [30, 31, 32]), which is obtained by replacing the trapping potential $V(\mathbf{r})$ with the effective mean field potential $V(\mathbf{r}) + 2g\rho(\mathbf{r})$. We perform numerical HF calculations with our experimental parameters, and obtain critical numbers that are only ~ 2 times larger than $N_{c,id}$, which is still far from the experimentally found ratio $\alpha = 5.3$. We also note that the HF profile, numerically propagated in time of flight, is clearly distinguishable from the experimentally observed distributions. This suggests that taking interactions into account at the mean field level is insufficient [33]. Motivated purely by our experimental observations, we introduce a second model in which the critical in-trap distribution is Gaussian, with a peak density ρ_c (Eq. 2) and widths σ_i ($i = x, y$) given by

$m\omega_i^2\sigma_i^2 = kT$. This leads to a simple result:

$$N_{\rm c,BKT} = \rho_{\rm c}\lambda^2 \left(\frac{kT}{\hbar\bar{\omega}}\right)^2 = \rho_{\rm c}\lambda^2 \frac{6}{\pi^2} N_{\rm c,id} \ . \qquad (3)$$

For our parameters the BKT threshold is given by $\rho_{\rm c}\lambda^2 = 8.0$, corresponding to $N_{\rm c,BKT}/N_{\rm c,id} = 4.9$. This is similar to the experimental ratio $\alpha = 5.3$.

In conclusion, we have shown that the ideal gas theory, which is very successful in predicting the critical point for 3D Bose-Einstein condensation, is inapplicable in 2D. In an interacting 2D Bose gas, we find the critical atom number for the onset of both bimodality and coherence to be ~ 5 times higher than expected for ideal gas condensation. This demonstrates that in 2D interactions play a profound role even in the normal state. A heuristic model based on the BKT theory of superfluidity and the experimentally observed density profiles provides a much better prediction of the critical point. We have also shown that the low temperature state displays properties largely analogous to those of 3D BECs. In particular, the narrow component of the bimodal time-of-flight density distributions follows the Thomas-Fermi law characteristic of superfluid hydrodynamics, and shows coherence in interference experiments. The only qualitative difference is the absence of true long-range order [13].

Finally, it is worth noting that in the strongly interacting 2D helium superfluid [1] the value of the coupling constant is estimated to be $\tilde{g} \sim 1$ [26], while in earlier experiments with sodium atoms $\tilde{g} \sim 10^{-2}$ [6]. In our experiments with $\tilde{g} \sim 10^{-1}$ we realized an intermediate regime of moderately strong interactions. In future experiments with atomic gases, a range of coupling strengths from $\tilde{g} = 1$ to $\tilde{g} = 10^{-4}$ could realistically be explored with the use of a Feshbach resonance, allowing for detailed quantitative tests of the microscopic BKT theory.

Z.H. and P.K acknowledge support from the EU (Contracts MIF1-CT-2005-007932 and MEIF-CT-2006-025047). This work is supported by Région Ile de France (IFRAF), CNRS, the French Ministry of Research, and ANR. Laboratoire Kastler Brossel is a research unit of Ecole Normale Supérieure and Université Paris 6, associated to CNRS.

[1] D. J. Bishop and J. D. Reppy, Phys. Rev. Lett. **40**, 1727 (1978).
[2] V. L. Berezinskii, Sov. Phys. JETP **34**, 610 (1972).
[3] J. M. Kosterlitz and D. J. Thouless, J. Phys. C: Solid State Physics **6**, 1181 (1973).
[4] N. D. Mermin and H. Wagner, Phys. Rev. Lett. **17**, 1133 (1966).
[5] P. C. Hohenberg, Phys. Rev. **158**, 383 (1967).
[6] A. Görlitz *et al.*, Phys. Rev. Lett. **87**, 130402 (2001).
[7] S. Burger, F. S. Cataliotti, C. Fort, P. Maddaloni, F. Minardi, and M. Inguscio, Europhys. Lett. **57**, 1 (2002).
[8] D. Rychtarik, B. Engeser, H.-C. Nägerl, and R. Grimm, Phys. Rev. Lett. **92**, 173003 (2004).
[9] Z. Hadzibabic, S. Stock, B. Battelier, V. Bretin, and J. Dalibard, Phys. Rev. Lett. **93**, 180403 (2004).
[10] N. L. Smith, W. H. Heathcote, G. Hechenblaikner, E. Nugent, and C. J. Foot, Journal of Physics B **38**, 223 (2005).
[11] M. Köhl, H. Moritz, T. Stöferle, C. Schori, and T. Esslinger, J. Low Temp. Phys. **138**, 635 (2005).
[12] S. Stock, Z. Hadzibabic, B. Battelier, M. Cheneau, and J. Dalibard, Phys. Rev. Lett. **95**, 190403 (2005).
[13] Z. Hadzibabic, P. Krüger, M. Cheneau, B. Battelier, and J. Dalibard, Nature **441**, 1118 (2006).
[14] I. B. Spielman, W. D. Phillips, and J. V. Porto, Phys. Rev. Lett. **98**, 080404 (2007).
[15] D. S. Petrov, M. Holzmann, and G. V. Shlyapnikov, Phys. Rev. Lett. **84**, 2551 (2000).
[16] D. S. Petrov and G. V. Shlyapnikov, Phys. Rev. A **64**, 012706 (2001).
[17] J. O. Andersen, U. Al Khawaja, and H. T. C. Stoof, Phys. Rev. Lett. **88**, 070407 (2002).
[18] T. P. Simula and P. B. Blakie, Phys. Rev. Lett. **96**, 020404 (2006).
[19] M. Holzmann, G. Baym, J.-P. Blaizot, and F. Laloë, Proc. Natl. Acad. Sci. USA **104**, 1476 (2007).
[20] V. Bagnato and D. Kleppner, Phys. Rev. A **44**, 7439 (1991).
[21] D. R. Nelson and J. M. Kosterlitz, Phys. Rev. Lett. **39**, 1201 (1977).
[22] A. Polkovnikov, E. Altman, and E. Demler, Proc. Natl. Acad. Sci. USA **103**, 6125 (2006).
[23] F. S. Dalfovo, L. P. Pitaevkii, S. Stringari, and S. Giorgini, Rev. Mod. Phys. **71**, 463 (1999).
[24] F. Gerbier, J. H. Thywissen, S. Richard, M. Hugbart, P. Bouyer, and A. Aspect, Phys. Rev. Lett. **92**, 030405 (2004).
[25] D. S. Fisher and P. C. Hohenberg, Phys. Rev. B **37**, 4936 (1988).
[26] N. Prokof'ev, O. Ruebenacker, and B. Svistunov, Phys. Rev. Lett. **87**, 270402 (2001).
[27] Y. Kagan, B. V. Svistunov, and G. V. Shlyapnikov, Sov. Phys. JETP **66**, 314 (1987).
[28] Note that the slope dN_0/dN for $N > N_{\rm c}$ is less than unity, contrary to what is expected for a saturated gas. This lack of saturation will be discussed elsewhere.
[29] Y. Shin, M. Saba, A. Schirotzek, T. A. Pasquini, A. E. Leanhardt, D. E. Pritchard, and W. Ketterle, Phys. Rev. Lett. **92**, 150401 (2004).
[30] R. K. Bhaduri, S. M. Reimann, S. Viefers, A. Ghose Choudhury, and M. K. Srivastava, J. Phys. B: At. Mol. Opt. Phys. **33**, 3895 (2000).
[31] J. P. Fernández and W. J. Mullin, J. Low Temp. Phys. **128**, 233 (2002).
[32] C. Gies and D. A. W. Hutchinson, Phys. Rev. A **70**, 043606 (2004).
[33] N. Prokof'ev and B. Svistunov, Phys. Rev. A **66**, 043608 (2002).